Journal of Electrical and Electronics Engineering (IOSR-JEEE)
e-ISSN: 2278-1676, p-ISSN: 2320-3331, Volume 21, Issue 4 Ser. 1 (July. – August. 2026), PP 26-34
www.iosrjournals.org

Synergetic Control Synthesis For A DC Electric Drive System

Tang Thanh Lam, To Xuan Dinh, Nguyen Ngoc Tuan
Institute Of Control Engineering, Le Quy Don Technical University, Hanoi, Vietnam

Abstract:
This study presents the application of synergetic control theory to the synthesis of a speed-controlled DC electric drive system. Two synthesis approaches were considered. The first approach is based on the system of equations describing a DC motor with the load torque represented as a function of speed, without explicitly considering disturbances. The second approach takes load disturbances into account by augmenting the original system of equations with an additional equation describing the disturbance dynamics. The simulation results were compared with those of drive systems synthesized using the modulus optimum, symmetrical optimum criteria and the linear quadratic regulator, thereby highlighting the advantages and limitations of the respective approaches.
Keywords: *DC motor control; Synergetic control; Motor speed stabilization.*

Date of Submission: 16-07-2026 Date of Acceptance: 26-07-2026

I. Introduction

DC drive systems are widely used owing to their good dynamic performance, ease of control, and suitability for a wide range of applications. DC motors are also frequently used as standard second-order control objects in research models for the development and performance evaluation of modern control laws. Methods for synthesizing DC electric drive systems can be broadly classified into two major groups: linear control methods, including synthesis based on the modulus optimum and symmetrical optimum criteria, modal control, and the linear quadratic regulator (LQR); and nonlinear, adaptive, and intelligent control methods.

According to the classical linear approach [1], a DC electric drive system is structured as a set of control loops. The inner current control loop is synthesized according to the modulus optimum criterion. The speed control loop is synthesized according to either the modulus optimum or the symmetrical optimum criterion. The controllers (control laws) in these loops are typically of the PID type.

The LQR is formulated by minimizing an objective functional of the following form [2]:

$$J = \int_0^\infty (x^T Q x + u^T R u)dt \qquad (1)$$

where x is the state vector, u is the control vector, Q is a symmetric, positive-semidefinite state-weighting matrix, and R is a symmetric, positive definite control-weighting matrix.

By solving the algebraic Riccati equation, the state-feedback gain vector **K** is determined, yielding the optimal control law **u = −Kx**.

The main advantage of LQR is that it simultaneously ensures satisfactory transient performance and limits the control amplitude, thereby providing a balance between the response speed and control energy consumption. However, LQR requires an accurate and complete mathematical model of the system. Moreover, the selection of the weighting matrices Q and R is still mostly heuristic, relying on designer experience or assisted by optimization algorithms, with no universal tuning rule available.

In practice, a DC motor is a control object characterized by various nonlinear factors, including magnetic circuit saturation; the influence of various types of friction; permissible limits on armature voltage and motor current; and variations in the resistance, inductance, load torque, and other parameters. Therefore, numerous nonlinear, adaptive, and intelligent control schemes have been proposed and implemented to improve control performance. Sliding-mode, fuzzy, adaptive, and backstepping control methods each offer specific advantages, but all aim to improve the robustness and adaptability of the system in the presence of model uncertainties and external disturbances.

Among the various available approaches, the basic synergetic control method, known as the Analytical Design of Aggregated Regulators (ADAR) method, represents a promising solution for implementation. Synergetic control theory was developed by Kolesnikov A.A. [3] and his collaborators, including Popov A.N., Kuz'menko A.A., Veselov G.E., and Kolesnikov A.Al. at Southern Federal University, Russia. This theory has been applied to nonlinear and complex control problems [4] in a wide range of fields, including power electronics

[5, 6], electromechanical systems and electric drives [7], and turbine-generator system control [8, 9]. The synergetic control problem is formulated as follows [3, 10]:

The control object is described by the following vector-matrix differential equation:

$$\dot{x}(t) = f(x) + G(x)u \tag{2}$$

Here, $x = (x_1, ..., x_n)^T$ is the state vector, $u = (u_1, ..., u_m)^T$ is the control vector, $f(x) = (f_1(x), ..., f_n(x))T$ is a vector of functions, and $G(x) = (g_{ij}(x))_{n\times m}$ is a matrix of functions.

It is necessary to determine a scalar or vector control law $u = u(x)$ that ensures that the representative point of system (2) moves from an arbitrary initial state (in some allowed area) to the manifolds $\psi_k(x) = 0$ and subsequently evolves along these manifolds toward a specified state, particularly the origin point $x = 0$ of the state space. The motion of the representative point must satisfy the fundamental functional equations of the ADAR method:

$$T_k\dot{\psi}_k(t) + \varphi(\psi_k) = 0 \tag{3}$$

The functions $\varphi_k(\psi_k)$ are selected so that, in addition to ensuring asymptotic stability, they provide the desired control performance characteristics.

The synergetic control problem can be formulated as an optimal control problem. Equations (3) are the Euler–Lagrange equations of the generalized conjugate functional [10, 11]:

$$J = \int_0^\infty \left[\varphi_k^2(\psi_k) + T_k^2\dot{\psi}_k^2(t)\right]dt = 0 \tag{4}$$

Here, $\varphi_k(\psi_k)$ is a single-valued, continuous, differentiable function $\forall\psi_k$; $\varphi_k(0) = 0$; $\varphi_k(\psi_k).\psi_k > 0 \ \ \forall\psi_k \neq 0$.

Therefore, the scalar or vector control law $u = u(x)$ synthesized using the ADAR method ensures that functional (4) attains its minimum. However, unlike the LQR method, functional (4) plays only a secondary role here and does not directly participate in the control law synthesis procedure. A detailed description of the theoretical background and design procedure for the ADAR method is presented in [3, 4].

Synergetic control exhibits interesting characteristics when compared with sliding-mode control, LQR, and backstepping control. Reference [5] analyzes and compares sliding-mode control with synergetic control. Reference [10] presents comparisons between synergetic control and LQR. Reference [12] demonstrates the advantages of synergetic control over backstepping control. In an illustrative case, when appropriate coefficients are selected, the synthesized control laws obtained using synergetic control and backstepping control are identical. Synergetic control is a general method and can even provide better results than backstepping control [12].

II. Synergetic Control Synthesis

There are two main types of DC motors: wound-field (separately excited) DC motors and permanent-magnet (PM) DC motors. In the wound-field type, the flux can be adjusted by varying the field current, whereas in the PM type, the flux is fixed and cannot be changed. Consequently, the wound-field DC motor has two control inputs: the armature voltage and the field voltage. In contrast, the PM DC motor has only one control input, namely the armature voltage. In principle, flux weakening is only possible in the direction of reducing the flux below its rated value and is typically employed in the speed region above the base speed. In the speed range up to the base speed, the flux is maintained constant at its rated value. If the motor operates only in the speed range up to the base speed, the field winding can be connected to a constant voltage. In this case, control is performed through the armature voltage, similarly to a PM DC motor. To obtain a general control law applicable to both motor types, only armature voltage control is considered here, while the flux is held constant.

The motor torque equation is given by:

$$M = M_c(\omega) + J_{eq}\frac{d\omega}{dt} \tag{5}$$

where $\mathbf{M = K_t\, i}$ is the electromagnetic torque of the motor (Nm), $\mathbf{K_t}$ is the torque constant (Nm/A), $\boldsymbol{\omega}$ is the angular speed of the motor (rad/s), **i** is the armature current (A), $\mathbf{M_c(\omega)}$ is the load torque, which is a function of angular speed, $\mathbf{J_{eq}}$ is the equivalent moment of inertia of the mechanical system referred to the motor shaft (Nms²/rad).

Dividing both sides by J_{eq} gives:

$$\frac{d\omega}{dt} = -\frac{M_c(\omega)}{J_{eq}} + \frac{K_t}{J_{eq}}i \tag{6}$$

The voltage balance equation of the DC motor is:

$$u = Ri + e + L\frac{di}{dt} \tag{7}$$

where $e = K_e \omega$ is the armature back-EMF (V), K_e is the back-EMF constant (Vs/rad), **u** is the armature voltage (V), **R** is the armature resistance (Ω), **L** is the armature inductance (H).

$$\frac{di}{dt} = -\frac{R}{L}i - \frac{K_e}{L}\omega + \frac{1}{L}u \qquad (8)$$

Let the state variables be defined as $x_1 = \omega$, $x_2 = i$, and:

$$a_{11} = -\frac{1}{J_{eq}}; \quad a_{12} = \frac{K_t}{J_{eq}}; \quad a_{21} = -\frac{K_e}{L}; \quad a_{22} = -\frac{R}{L}; \quad b = \frac{1}{L}$$

From (6), (8), and the above notation, the following state-space model is obtained:

$$\begin{cases} \dot{x}_1 = a_{11}M_c(x_1) + a_{12}x_2 \\ \dot{x}_2 = a_{21}x_1 + a_{22}x_2 + bu \end{cases} \qquad (9)$$

The motor speed is the controlled variable and must be stabilized at the reference value x_{1ref}. We define the macro variable as:

$$\psi_1 = x_1 - x_{1ref} \qquad (10)$$

where x_1 is the angular speed of the motor, and x_{1ref} is the reference angular speed.

The functional equation of the ADAR method is:

$$T_1\dot{\psi}_1 + \psi_1 = 0 \qquad (11)$$

where $T_1 > 0$. T_1 is a design parameter that determines the convergence rate toward the invariant manifold defined by the macro variable.

Substituting (10) into (11) and combining the result with (9) yields:

$$x_2 = \frac{x_{1ref} - x_1}{a_{12}T_1} + \frac{a_{11}M_c(x_1)}{a_{12}} \qquad (12)$$

Here, the armature current is the control variable. Define the macro variable as:

$$\psi_2 = x_2 - \varphi(x_1) \qquad (13)$$

The functional equation of the ADAR method is:

$$T_2\dot{\psi}_2 + \psi_2 = 0 \qquad (14)$$

where $T_2 > 0$. T_2 is a design parameter that determines the convergence rate toward the invariant manifold defined by the macro variable.

Substituting (13) into (14) yields:

$$T_2\left[\dot{x}_2 - \frac{d\varphi(x_1)}{dt}\right] + x_2 - \varphi(x_1) = 0 \qquad (15)$$

When $\psi_2 \to 0$, $x_2 \to \varphi(x_1)$. Substituting (12) into (15) and solving for the control variable gives:

$$u = \frac{1}{b}\left\{ \frac{1}{a_{12}T_1T_2}\left(x_{1ref} - x_1\right) + \frac{a_{11}M_c(x_1)}{a_{12}T_2} + a_{21}x_1 + \left(a_{22} - \frac{1}{T_2}\right)x_2 + \right. \\ \left. + \left[-a_{11}M_c(x_1) + a_{12}x_2\right]\left[\frac{a_{11}}{a_{12}}\frac{dM_c(x_1)}{dx_1} - \frac{1}{a_{12}T_1}\right]\right\} \qquad (16)$$

When load disturbances are considered, the torque equation of the motor is given by:

$$M = M_c(\omega) + M_f(t) + J_{eq}\frac{d\omega}{dt} \qquad (17)$$

where $M_f(t)$ denotes the applied load disturbance torque.

According to the integral adaptation method [8, 9], the effects of external disturbances on system operation are compensated for by nonlinear control laws incorporating specially structured integral elements in the feedback paths. In this approach, only minimal information about the disturbance and its form (piecewise constant, polynomial, harmonic, etc.) is required. The disturbance can then be represented by an approximate dynamic model in the form of a system of differential equations. Synergetic control based on the integral adaptation principle provides disturbance adaptation without requiring the design of a complex observer. At the point where the disturbance acts, an auxiliary variable $z_1(t)$ is introduced. This variable represents an estimate of the disturbance: $\hat{z}_1 = M_f(t)$. The original system of differential equations is augmented with an equation describing the disturbance dynamics.

From (9), the resulting extended state space model is:

$$\begin{cases} \dot{x}_1 = a_{11}(M_c(x_1) + z_1) + a_{12}x_2 \\ \dot{x}_2 = a_{21}x_1 + a_{22}x_2 + bu \\ \dot{z}_1 = \beta(x_1 - x_{1ref}) \end{cases} \quad (18)$$

Here, the armature current is the control variable and $\beta > 0$. Define the macro variable as:

$$\psi_3 = x_2 - \varphi_3(x_1, z_1) \quad (19)$$

Function $\varphi_3(x_1, z_1)$ is referred to as the internal control law. This function ensures the control objective and determines the evolution of the armature current on manifold $\psi_3 = 0$.

Solving the functional equation of the ADAR method yields:

$$T_3\dot{\psi}_3 + \psi_3 = 0 \quad (20)$$

where $T_3 > 0$. T_3 is a design parameter that determines the convergence rate toward the manifold defined by the macro variable.

Substituting (19) into (20) yields:

$$T_3\left[\dot{x}_2 - \dot{\varphi}_3\right] + x_2 - \varphi_3 = 0 \quad (21)$$

where:

$$\dot{\varphi}_3(x_1, z_1) = \frac{\partial \varphi_3}{\partial x_1}\dot{x}_1 + \frac{\partial \varphi_3}{\partial z_1}\dot{z}_1 = \\ = \frac{\partial \varphi_3}{\partial x_1}\left[a_{11}(M_c(x_1) + z_1) + a_{12}x_2\right] + \frac{\partial \varphi_3}{\partial z_1}\beta\left(x_1 - x_{1ref}\right) \quad (22)$$

Substituting the expressions from (18) and (22) into (21) and solving for the control variable yields:

$$u = -\frac{a_{21}}{b}x_1 - \frac{a_{22}}{b}x_2 + \frac{1}{b}\left\{\frac{\partial \varphi_3}{\partial x_1}\left[a_{11}(M_c + z_1) + a_{12}x_2\right] + \frac{\partial \varphi_3}{\partial z_1}\beta\left(x_1 - x_{1ref}\right)\right\} + \\ + \frac{1}{bT_3}\left[\varphi_3(x_1, z_1) - x_2\right] \quad (23)$$

On the invariant manifold $\psi_3 = 0$, $x_2 = \varphi_3(x_1, z_1)$. Therefore, the motion along the invariant manifold $\psi_3 = 0$ is described as follows:

$$\dot{x}_{1\psi_3} = a_{11}(M_c(x_{1\psi_3}) + z_1) + a_{12}\varphi_3(x_{1\psi_3}, z_1) \quad (24)$$

If the following is selected:

$$\varphi_3(x_1, z_1) = -\frac{1}{a_{12}}\left[a_{11}(M_c(x_1) + z_1) + K(x_1 - x_{1ref})\right] \quad (25)$$

then

$$\dot{x}_1 = -K(x_1 - x_{1ref}) \quad (26)$$

For $K > 0$, (26) is asymptotically stable, and $x_1 \rightarrow x_{1ref}$ as time increases.

From (25), we obtain:

$$\frac{\partial \varphi_3}{\partial x_1} = -\frac{1}{a_{12}}\left[a_{11}\frac{\partial M_c}{\partial x_1} + K\right]; \quad \frac{\partial \varphi_3}{\partial z_1} = -\frac{a_{11}}{a_{12}} \quad (27)$$

Substituting (25), (27), and z_1 from (18) into (23) yields:

$$u=-\frac{a_{21}}{b}x_1-\frac{a_{22}}{b}x_2-\frac{1}{a_{21}}\left[\left(a_{11}\frac{\partial M_c}{\partial x_1}+K\right)\left(\frac{a_{21}}{b}x_2+M_c\right)+\beta\left(x_1-x_{1ref}\right)\right]-$$
$$-\frac{\beta}{a_{21}}\left[\frac{1}{T_3}+a_{11}\frac{\partial M_c}{\partial x_1}+K\right]\int\left(x_1-x_{1ref}\right)dt-\frac{1}{a_{21}T_3}\left[M_c+\frac{K}{a_{11}}\left(x_1-x_{1ref}\right)\right]-\frac{x_2}{bT_3} \tag{28}$$

III. Simulation And Discussion

The simulation study was carried out on a DC motor with the following parameters:

P_n = 37.3 kW; U_n = 240 V; n = 1750 rpm; M_n = 203.5 Nm; I_n = 174.6 A; J = 0.2053 kgm²; K_t = 1.2033 Nm/A; K_e = 1.2033 Vs/rad; R = 0.1113 Ω; L = 0.001558 H.

Figure 1 shows the speed and current responses of the motor when the reference speeds are 400, 1000, and 1750 rpm, respectively. In this case, the control law (16) is used. For step changes in the load torque of ±20% of the rated value, the motor current responds accordingly, while the speed deviates temporarily from its steady-state value (corresponding to the reference speed). After a transient period, the motor speed returns to the reference value. The system is stable and is capable of maintaining the reference speed with zero steady-state error.

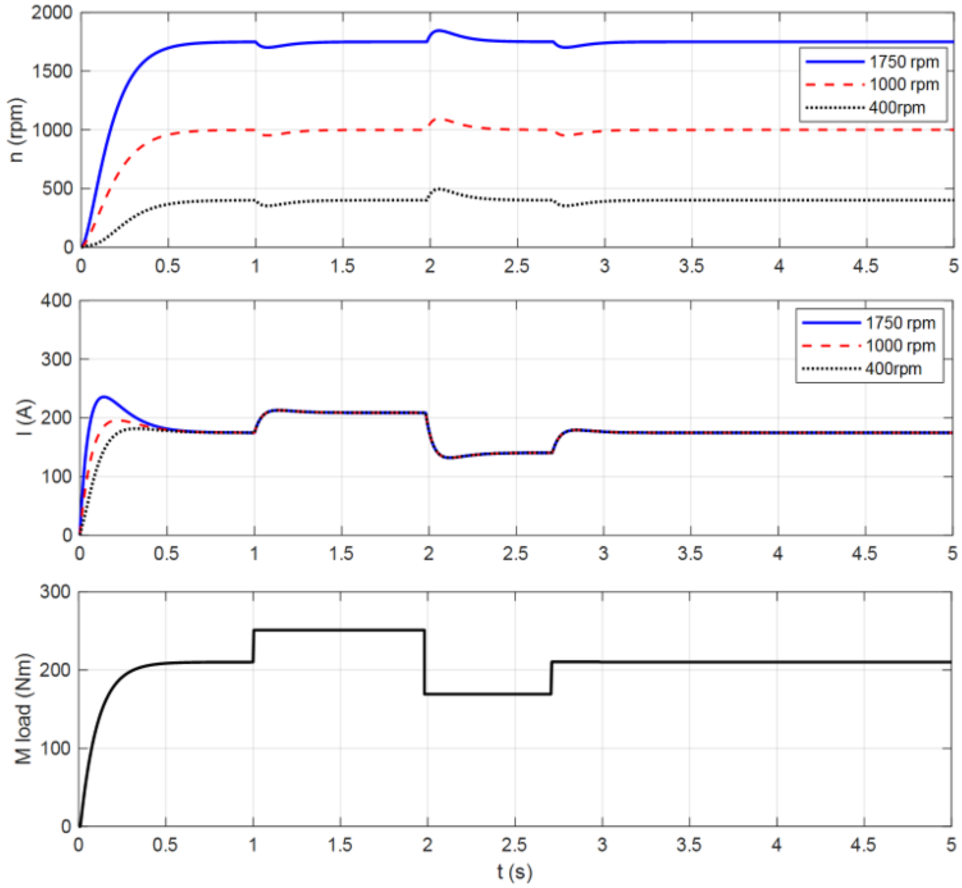

Figure 1. Speed and current responses of the motor under the control law (16)

Figure 2 illustrates the speed and current responses when the reference speeds were set to 400, 1000, and 1750 rpm, but with the control law (28) applied. Under step changes in the remaine (±20% of the rated torque), the motor current changed correspondingly. In comparison with those of (16), the responses achieved under control law (28) are significantly improved. Specifically, the motor speed deviated only slightly under load torque disturbances. The system remained stable and maintained the reference speed with zero steady-state error.

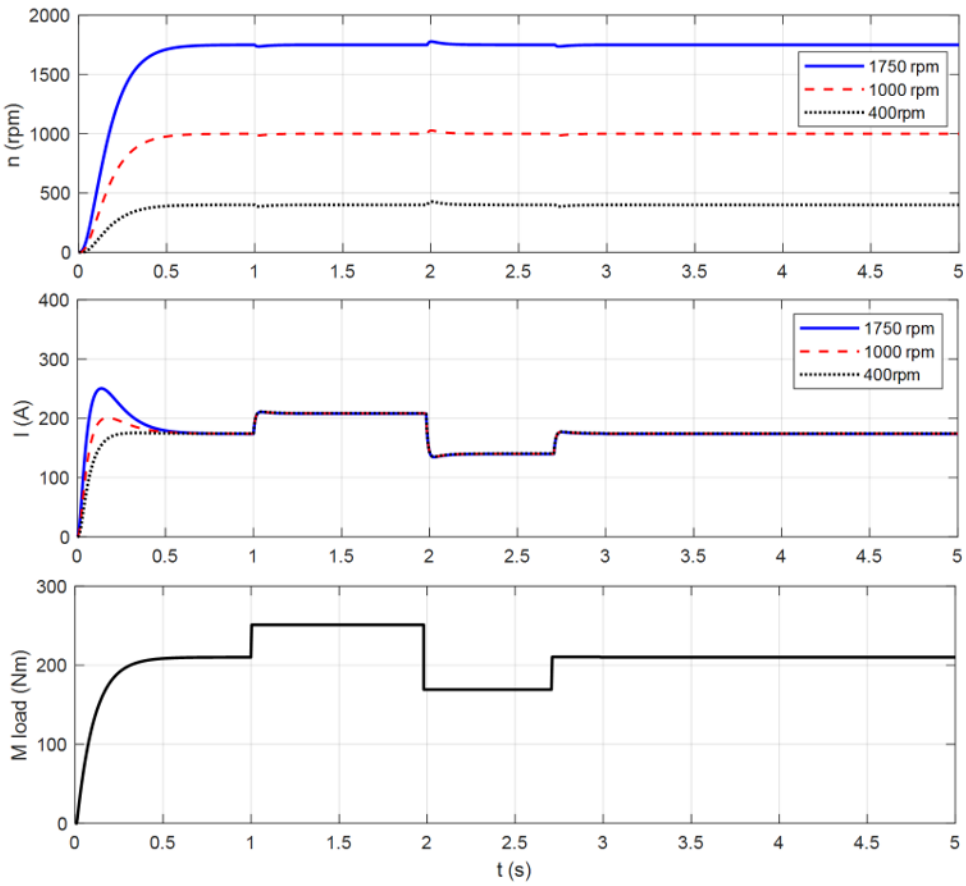

Figure 2. Speed and current responses of the motor under the control law (28)

Figures 3 and 4 present the speed and current responses during motor startup under four different control methods. All systems were evaluated at the same speed setpoint of 1750 rpm and rated load torque $M_n = 203.5$ Nm.

The four control laws are as follows:

1) Two-loop (current and speed) PI control: The inner current loop is designed according to the Modulus Optimum (MO) criterion as a PI controller of the form:

$$W_r(s) = K_r + \frac{1}{T_r s} \tag{29}$$

with parameters $K_r = 0.1623$ and $T_r = 0.0863$ s.

The outer speed loop was designed according to the Symmetrical Optimum (SO) criterion as a PI controller of the form (29), with parameters $K_r = 6.8246$ and $T_r = 0.0059$. The responses of this system are denoted as MO-SO.

2) Linear quadratic regulator control: The control law minimizes the quadratic cost function (1). The responses are denoted as LQR, where:

$$R = 0.1; \quad Q = \begin{bmatrix} 0.1 & 0 \\ 0 & 0.01 \end{bmatrix}$$

The state-feedback gain vector is given by: $K = R^{-1}B^T P$

$$A = \begin{bmatrix} a_{11} & a_{12} \\ a_{21} & a_{22} \end{bmatrix} = \begin{bmatrix} -0.0343 & 5.8612 \\ -772.3363 & -71.4377 \end{bmatrix}; \; B = \begin{bmatrix} 0 \\ 641.8485 \end{bmatrix}; \; C = \begin{bmatrix} 1 & 0 \end{bmatrix}; \; D = 0.$$

$$K = \begin{bmatrix} 0.3598 & 0.2336 \end{bmatrix}.$$

The weighting matrices Q and R are selected based on engineering experience. The computation of the state-feedback gain vector K and evaluation of the system responses were performed using MATLAB/Simulink.

3) Analytical Design of Aggregated Regulator 1 (ADAR1): Based on control law (16), with parameters $b = 641.8485$, $T_1 = 0.05$, $T_2 = 0.1$. The responses are denoted as ADAR1.

4) Analytical Design of Aggregated Regulator 2 (ADAR2): Based on control law (28), with parameters $b = 641.8485$, $T_3 = 0.01$, $\beta = 0.05$, $K = 15$. The responses are denoted as ADAR2.

During startup, the speed and current responses obtained with the ADAR1 and ADAR2 control laws are similar, with both exhibiting longer rise times than those obtained with the LQR and PI (MO-SO) controllers. In the MO-SO case, a very large current overshoot was observed. To limit the startup current in the MO-SO system, a saturation block is typically inserted at the input of the current loop reference. Due to the nonlinear nature of the saturation, the response of the system within the saturation region is difficult to predict and determine.

The LQR control law was implemented using the selected weighting matrices R and Q. The motor speed and current responses during startup exhibited rapid and smooth transients. The peak current was approximately twice the rated current, which was within the permissible limits for most DC motors.

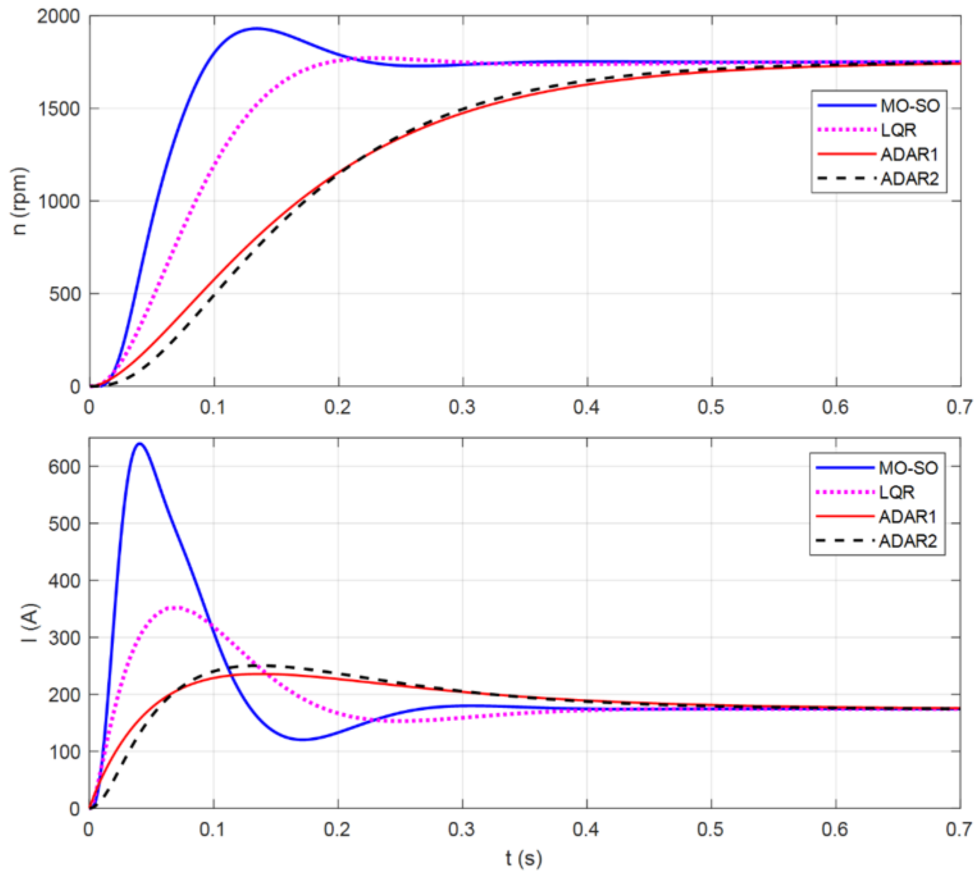

Figure 3. Transient responses during startup under different control laws

Figure 4 shows the speed and current variations under load torque disturbances. At $t = 2$ s, the load torque suddenly decreased from $1.2M_n$ to $0.8M_n$. At $t = 2.7$ s, the load torque increased from $0.8M_n$ to M_n, corresponding to the rated current $I_n = 174.6$ A. The motor current responded rapidly to these step changes. As shown in the upper plots of Figure 4, the speed deviation was smallest, and the fastest recovery was achieved using the ADAR2 control law. Under abrupt decreased or increased in the load torque, both the ADAR1 and LQR controllers exhibited similar speed deviations, but the LQR controller recovers to its steady-state speed faster than ADAR1. The two-loop control system designed based on the MO-SO criteria exhibited good disturbance rejection performance under abrupt variations in load torque. All four control laws ensured stability and the ability to maintain the reference speed of 1750 rpm.

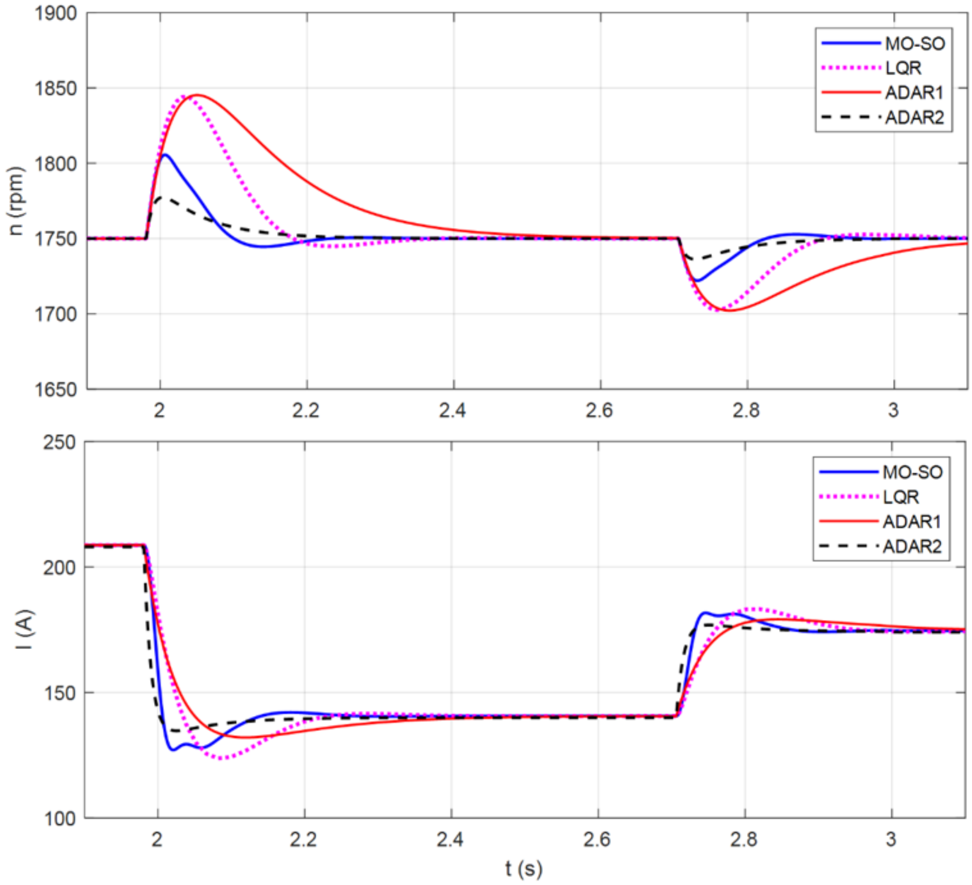

Figure 4. Motor responses under step changes in load torque for different control laws

IV. Conclusion

This study presents two design approaches for speed-controlled DC drive systems based on synergetic control theory. The control laws are expressed in an analytical form and represent optimal control according to (4). Both control laws ensure stability and the ability to maintain the reference speed in the presence of sudden step-type load disturbances. The transient responses of speed and current during startup are similar for both control laws. The smooth rise in speed and current is a key advantage of these methods. The startup current does not exceed the permissible value, unlike what is typically encountered when using the modulus optimum and symmetrical optimum criteria. Comparative results obtained with conventional PI controllers designed by MO-SO, as well as with the LQR, are also provided. Under abrupt load changes, the control law (28) demonstrates a fast dynamic response and offers the best speed regulation performance among all compared methods. However, a common drawback of the two ADAR designs is the relatively high complexity of the control laws.

References

[1]. Basharin A.V., Novikov V.A., Sokolovsky G.G. Electric Drive Control, Energoizdat, 1982.
[2]. Naidu D.S. Optimal Control Systems, CRC Press LLC, 2003.
[3]. Kolesnikov A.A. Synergetic Control Theory, Moscow, Energoavtomizdat, 1994.
[4]. Kolesnikov A.A. Synergetic Methods For Controlling Complex Systems: Energy Systems, Moscow: Komkniga, 2006.
[5]. Santi E., Monti A., Li D., Proddutur K., Dougal R. Synergetic Control For Power Electronics Applications: A Comparison With The Sliding Mode Approach, Ejournal Of Circuits, Systems, And Computers, Vol. 13, No. 4 (2004) 737-760. World Scientific Publishing Company.
[6]. Kolesnikov A.A., Veselov G., Monti A., Ponci F., Santi E., Dougal R. Synergetic Synthesis Of Dc-Dc Boost Converter Controllers: Theory And Experimental Analysis, IEEE Applied Power Electron. Conf. (APEC 2002), 10-14 March 2002, Dallas, Texas, Pp. 409-415.
[7]. Popov A.N. Synergetic Synthesis Of Energy-Saving Control Laws For Electromechanical Systems, Taganrog: Publishing House Of TRTU, 2003.
[8]. Kuz'menko A.A. Nonlinear Synthesis Of An Adaptive Control Law For The Rotational Speed Of A Hydraulic Turbine: Integral Adaptation, Problems Of Power Engineering, 2015, No. 1–2.
[9]. Kuz'menko A.A., Sinitsyn A.S., Kolesnichenko D.A. The Principle Of Integral Adaptation In The Problem Of Adaptive Control Of A "Hydraulic Turbine–Synchronous Generator" System, Control Systems And Information Technologies, 2014, No. 2-1 (56), Pp. 146–150.
[10]. Kolesnikov A.A., Kolesnikov Al.A., Kuz'menko A.A. The ADAR And LQR Methods In The Problems Of Synthesis Of The Nonlinear Control Systems, Mekhatronika, Avtomatizatsiya, Upravlenie, 2016, Vol. 17, No. 10, Pp. 657-669.

[11]. Kolesnikov S.I. Synthesis Of A Control System For A Second-Order Nonlinear Plant With Incomplete Description, Automation And Remote Control, 2018, No. 9.
[12]. Kolesnikov A.A., Kolesnikov Al.A., Kuz'menko A.A. The ADAR And Backstepping Methods In The Synthesis Of Nonlinear Control Systems, Mekhatronika, Avtomatizatsiya, Upravlenie, Vol. 17, No. 7, 2016.
[13]. Kolesnikov A.A., Kolesnikov Al.A., Kuz'menko A.A. The ADAR Method And Adaptive Control Theory In The Synthesis Of Nonlinear Control Systems, Mekhatronika, Avtomatizatsiya, Upravlenie, Vol. 18, No. 9, 2017.